MOLECULAR AND CELLULAR BIOLOGY, Mar. 2002, p. 1723–1733 Vol. 22, No. 6
0270-7306/02/$04.00+0 DOI: 10.1128/MCB.22.6.1723–1733.2002

Promoter Scanning for Transcription Inhibition with DNA-Binding Polyamides

Jennifer A. Ehley,[1] Christian Melander,[2] David Herman,[2] Eldon E. Baird,[2] Heather A. Ferguson,[3] James A. Goodrich,[3] Peter B. Dervan,[2]* and Joel M. Gottesfeld[1]*

Department of Molecular Biology, The Scripps Research Institute, La Jolla, California 92037[1]; Division of Chemistry and Chemical Engineering, California Institute of Technology, Pasadena, California 91125[2]; and Department of Chemistry and Biochemistry, University of Colorado at Boulder, Boulder, Colorado 80309[3]

Received 13 August 2001/Returned for modification 1 October 2001/Accepted 29 October 2001

When targeted to sequences adjacent to a TATA element, pyrrole-imidazole (Py-Im) polyamides inhibit the DNA binding activity of TATA box binding protein (TBP) and basal transcription by RNA polymerase II. In the present study, we scanned the human immunodeficiency virus type 1 promoter for polyamide inhibition of TBP binding and transcription using a series of DNA constructs in which a polyamide binding site was placed at various distances from the TATA box. Polyamide interference with either TBP-DNA or TFIID-TFIIA-DNA contacts both upstream and downstream of the TATA element resulted in inhibition of transcription. Our results define important protein-DNA interactions outside of the TATA element and suggest that transcription inhibition of selected gene promoters can be achieved with polyamides that target unique sequences within these promoters at a distance from the TATA element. Our studies also demonstrate the utility of the Py-Im polyamides for discovery of functionally important protein-DNA contacts involved in transcription.

Pyrrole-imidazole (Py-Im) polyamides are synthetic ligands that can be designed to bind predetermined DNA sequences (40, 44). These minor-groove DNA-binding molecules block eukaryotic transcription factors from binding to their cognate DNA sequences and inhibit transcription, both in vitro and, in a few cases, in cell culture experiments (reviewed in reference 13). Polyamides are effective inhibitors of tissue-specific and general transcription factors (7, 8) as well as viral repressors (9) and transactivators (29). Recently, activation of gene expression has been achieved in vitro by tethering a small peptide activation domain to a sequence-specific Py-Im polyamide (31). Remarkably, activation and repression of selected genes have been achieved in *Drosophila melanogaster* by targeting polyamides to highly repeated satellite DNA sequences (17, 18).

Since batteries of genes utilize common general and tissue-specific transcription factors, polyamides have been synthesized to bind sequences adjacent to the binding sites for required transcription factors (7). A polyamide targeted to sequences adjacent to the human immunodeficiency virus type 1 (HIV-1) TATA box effectively inhibits TATA box binding protein (TBP) binding and basal transcription by RNA polymerase II (7). The binding of the TBP subunit of TFIID in the minor groove nucleates assembly of the polymerase II transcription machinery for TATA-containing genes (24, 25). Since TFIID and the other general transcription factors TFIIA, -B, -E, -F, and -H (28, 33) occupy at least 40 bp of promoter DNA upstream from the transcription start site of mRNA-coding genes, this raises the question of whether sites nonoverlapping and distant from the TATA box might also serve as effective polyamide targets for inhibition of transcription. To address this issue, we generated a series of DNA constructs in which a common polyamide-binding site was scanned through a promoter and determined the effect of binding site position on inhibition of TBP binding and basal RNA polymerase II transcription. Our results show that essential protein-DNA contacts on the HIV-1 core promoter are not simply restricted to the TATA box and initiator element (20, 45) but rather extend both upstream and downstream of the TATA box. Some of these contacts are likely due to TFIID, the multiprotein complex containing TBP. Importantly, transcription inhibition can be achieved by targeting polyamides to promoter sequences distant from the TATA element that are gene specific. Py-Im polyamides thus provide simple and convenient chemical probes for discovery of functionally important protein-DNA contacts within specific gene promoters.

MATERIALS AND METHODS

Polyamide synthesis and characterization. Three Py-Im polyamides (1–3), whose structures are shown in Fig. 1A, were synthesized by solid-phase methods (1). Polyamide-EDTA conjugates were also prepared (40). The purity and identity of each compound were verified by analytical high-pressure liquid chromatography, ^{1}H nuclear magnetic resonance, and matrix-assisted laser desorption ionization–time of flight mass spectrometry (1). The polyamides were dissolved in distilled water and maintained as frozen stock solutions at approximately a 200 μM concentration. Polyamide concentrations were determined by measurement of UV absorbance at 308 nm using empirically determined extinction coefficients.

Site-directed mutagenesis. The sequence of the HIV-1 promoter contained within plasmid pLTR-CAT (35) was altered by oligonucleotide-directed mutagenesis in order to insert the binding site for a polyamide at various distances upstream and downstream from the TATA element. This was accomplished with the QuickChange mutagenesis kit from Stratagene and appropriate mutagenic oligonucleotides (Genosys, Woodlands, Tex.). In each instance, the mutagenic oligonucleotide contained polyamide-binding site sequence 5′-AGCTCGT-3′ and various lengths of wild-type HIV-1 flanking sequence. The oligonucleotides

* Corresponding author. Mailing address for Joel M. Gottesfeld: Department of Molecular Biology, The Scripps Research Institute, 10550 North Torrey Pines Rd., La Jolla, CA 92037. Phone: (858) 784-8913. Fax: (858) 784-8965. E-mail: joelg@scripps.edu. Mailing address for Peter B. Dervan: Division of Chemistry and Chemical Engineering, 164-30, California Institute of Technology, Pasadena, CA 91125. Phone: (626) 395-6002. Fax: (626) 683-8753. E-mail: dervan@cco.caltech.edu.

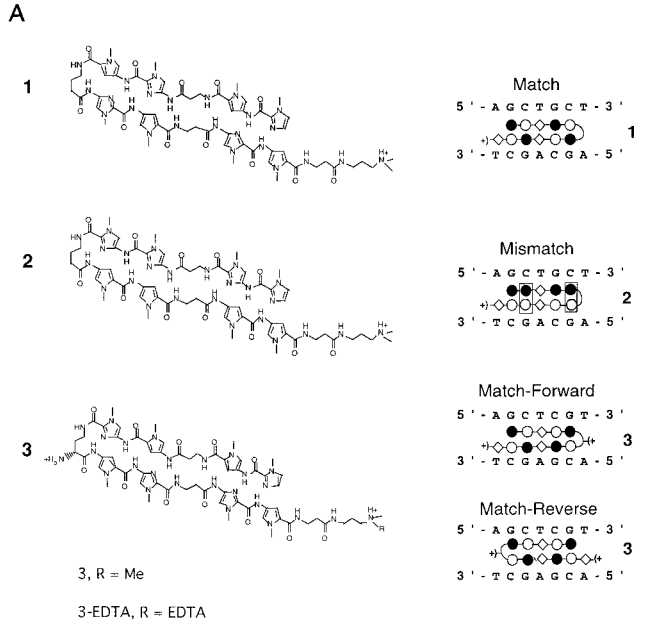

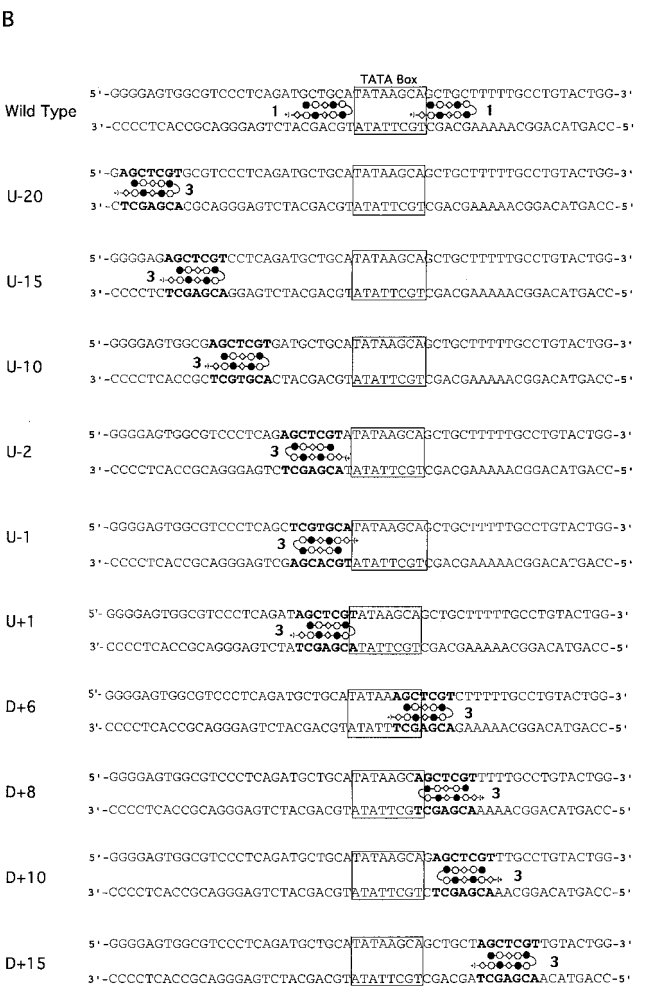

FIG. 1. Polyamide structures and binding sites. (A) Structures for polyamides ImPy-β-ImPy-γ-ImPy-β-ImPy-β-Dp (1), ImIm-β-ImIm-γ-PyPy-β-PyPy-β-Dp (2), and ImPy-β-PyIm-daba-PyIm-β-ImPy-β-Dp (3). Base sequence specificity depends on side-by-side pairing of Py and Im amino acids in the minor groove of DNA (6). Im-Py targets G·C base pairs and Py-Im targets C·G base pairs. Py-Py is degenerate and targets both A·T and T·A base pairs. The β-alanine–β-alanine pair also recognizes both A·T and T·A base pairs (42). Black and white circles, Im and Py rings, respectively; curved line, hairpin junction, which is formed with γ-aminobutyric acid or daba; diamonds, β-alanine; parenthesis with plus sign, Dp. The positive charge on the daba turn amino acid (3) is not shown. Me, methyl. (B) DNA sequences of the HIV-1 promoter constructs (from nucleotide positions −55 to +1, with respect to the transcription start site at +1), with polyamide binding sites at various distances upstream (U) or downstream (D) from the TATA box (boxed). Polyamide-binding models are shown.

ranged in length from 27 to 35 bases and were designed to minimize secondary structure effects with software obtained from the Genosys web site (www.genosys.com). The resulting clones were verified by DNA sequence analysis in the Scripps Core Facility.

DNase I footprint titrations and EMSA. Singly end-labeled DNA restriction fragments were derived from HIV-1 enhancer/promoter plasmid pLTR-CAT (35) and the polyamide-binding site derivatives which were generated by mutagenesis. These probes were labeled at the 3′ end of the top strand at the *Hin*dIII site, which is located at nucleotide position +80 within the HIV-1 coding sequence. Labeling with [α-^{32}P]dATP and Klenow DNA polymerase was carried out as recommended by the supplier (Roche Molecular Biosystems). After digestion with *Eco*RV (which cleaves at nucleotide position −340 from the transcription start site), the labeled 420-bp fragment was recovered from a nondenaturing polyacrylamide gel. Footprinting reaction mixtures contained approximately 1 ng of the labeled fragment in a 100-μl binding reaction mixture and yielded a DNA concentration of approximately 40 pM in a buffer containing 25 mM Tris-Cl, pH 8.0, 50 mM KCl, 0.1 mM dithiothreitol, 0.5 mM EDTA, 6.25 mM $MgCl_2$, 10% (vol/vol) glycerol, and 0.002% (vol/vol) NP-40. Binding reaction mixtures contained the final concentrations of polyamides indicated in the figure legends. Where indicated in the figure legends, recombinant human TBP (Promega) was included at a final concentration of 35 nM and recombinant TFIIA (a gift from Tae-Kyung Kim and D. Reinberg, University of Medicine and Dentistry of New Jersey) (37) was included at a final concentration of 216 nM. These concentrations were determined to be saturating in pilot titration experiments. Incubations were for the times indicated in the figure legends prior to digestion with 0.025 U of DNase I (Roche) for 30 s at 23°C. DNase I was diluted into the reaction buffer plus 1 mM $CaCl_2$. Reactions were stopped by the addition of sodium dodecyl sulfate and EDTA to final concentrations of 0.5% (wt/vol) and 25 mM, respectively. After extraction with phenol and ethanol precipitation, the samples were analyzed by electrophoresis on a 6% sequencing polyacrylamide gel containing 8.3 M urea, 88 mM Tris-borate, pH 8.3, and 2 mM EDTA. Quantitation of the footprint titrations was by storage phosphorimage analysis utilizing Kodak storage phosphor screens (SO 230) and a Molecular Dynamics SF PhosphorImager. The data were analyzed by using the ImageQuant software from Molecular Dynamics. Volume integration of the target site was corrected in each lane of the footprint gel by reference to a site in which the extent of DNase I digestion did not vary across either the TBP or polyamide titration. Site intensities were calculated after background subtraction, and binding affinities were determined using a nonlinear least-squares fitting procedure with KaleidaGraph software (version 3.0.1; Synergy Software). An electrophoretic mobility shift assay (EMSA) was used to assess inhibition of TFIID-TFIIA-DNA interactions. TFIID was purified from HeLa cells using an immunoaffinity isolation procedure (11). HeLa cell nuclear extracts were first fractionated by phosphocellulose chromatography (10), and proteins eluting between 0.5 and 1.0 M KCl were pooled. TFIID was further immunopurified using an anti-hTAFII130 monoclonal antibody. Immunoprecipitated material was washed extensively, and TFIID was specifically eluted from antibody beads with 2 column volumes of buffer containing an epitope peptide. Binding reaction mixtures contained 3 ng of the ^{32}P-labeled HIV-1 DNA fragments described above (yielding a final concentration of 0.6 nM in 20 μl) and empirically determined amounts of TFIID (at a 4 nM final concentration) and recombinant TFIIA (at a 240 nM final concentration) in a buffer consisting of 10 mM Tris-Cl, pH 7.9, 10 mM HEPES, pH 7.9, 10% glycerol, 6 mM $MgCl_2$, 50 mM KCl, 100 μg of bovine serum albumin/ml, and 1 mM dithiothreitol. DNA and polyamides

TABLE 1. Polyamide 3 binding affinities and inhibition constants

Construct	Site position relative to T+1	K_d (nM)[a]	TBP inhibition IC_{50} (nM)[b]	Relative transcription[c]	Transcription inhibition IC_{50} (nM)[d]
U−20	−26 to −20	ND[e]	>200[f]	0.79	50
U−15	−21 to −15	ND	>200	0.78	75
U−10	−16 to −10	4.0	>200	0.96	50
U−2	−8 to −2	4.6	17.5	1.10	25
U−1	−7 to −1	5.1	12.5	0.38	20
U+1	−6 to +1	6.0	10.0	<0.05	ND
D+6	+6 to +12	2.7	10.0	0.52	20
D+8	+8 to +14	4.7	35	0.65	50
D+10	+10 to +16	2.0	>200	0.41	>200
D+15	+15 to +21	ND	ND	0.97	75

[a] Determined by quantitative DNase footprinting under equilibrium conditions.
[b] Polyamide concentration required for half-maximal occupancy of TBP, as determined by DNase footprinting.
[c] Transcription in the absence of polyamides relative to wild type.
[d] Polyamide concentration required for 50% inhibition of transcription (see Fig. 7).
[e] ND, not determined.
[f] >200, no inhibition observed up to 200 nM polyamide.

were preincubated for 15 min at ambient temperature prior to the addition of TFIIA and TFIID. After a subsequent incubation for 20 min at 30°C, the reaction mixtures were subjected to electrophoresis on a nondenaturing 6% polyacrylamide gel containing 44 mM Tris-borate, pH 8.3, 1 mM EDTA, and 5 mM magnesium acetate and measuring 20 cm by 20 cm by 0.75 mm. Gels were prerun for 45 min and run for 3.5 h, both at 250 V at 4°C, with 44 mM Tris-borate, pH 8.3–1 mM EDTA–5 mM magnesium acetate as the electrophoresis buffer. Gels were dried and subjected to phosphorimage analysis.

Affinity cleavage reactions with polyamide 3-EDTA·Fe(II). Iron-mediated DNA cleavage under reducing conditions was performed as described previously (43). Briefly, reactions were performed by first incubating the desired concentrations of polyamide 3-EDTA with end-labeled DNA (40 pM final concentration) for 1 h in buffer consisting of 10 mM Tris-Cl, pH 7.6 and 20 mM NaCl, followed by addition of freshly prepared ferrous ammonium sulfate ($Fe[NH_4]_2[SO_4]_2 \cdot 6H_2O$) to a 10 μM final concentration. After incubation for 30 min, dithiothreitol was added to a final concentration of 10 mM, and the cleavage reaction was allowed to proceed for 10 min at ambient temperature. Reactions were terminated by the addition of EDTA to 25 mM, and the DNA was precipitated with ethanol and analyzed on a sequencing gel as described above.

Cell extracts, DNA templates, and in vitro transcription reactions. HeLa nuclear extract was purchased from Promega. Two microliters of extract and 100 ng of template DNA per 25-μl transcription reaction mixture were used as described previously (30). Runoff RNA transcripts of ~500 bases were obtained with *Eco*RI-digested plasmid DNA, and transcripts of ~200 bases were obtained with *Stu*I-digested DNA. Plasmid DNA was digested with these enzymes along with *Eco*RV, and the promoter-containing DNA fragments were purified from 0.8% agarose gels with the Qiagen QIAquick gel extraction kit. DNA concentrations were determined by ethidium staining of an analytical agarose gel by using known DNA concentrations as standards. Polyamide-DNA complexes were allowed to form at ambient temperature for 30 min prior to addition of extracts and other reaction components. After a subsequent incubation at 30°C for 1 h, transcription reactions were allowed to proceed for 45 min at 30°C. Reactions were stopped by the addition of an equal volume of a buffer containing 2% sodium dodecyl sulfate and 50 mM EDTA. After extraction with RNAzol (TelTest), RNA was precipitated with isopropanol and subjected to electrophoresis on a 6% polyacrylamide sequencing gel. The dried gels were subjected to phosphorimage analysis to estimate relative levels of RNA transcripts.

RESULTS

Inhibition of TBP binding with Py-Im polyamides. Previous studies established that polyamide 1 (ImPy-β-ImPy-γ-ImPy-β-ImPy-β-Dp [β, β-alanine; γ, γ-aminobutyric acid; Dp, dimethylaminopropylamide]; Fig. 1A), which binds upstream and downstream of the HIV-1 TATA element (Fig. 1B, wild type), inhibits TBP binding to the HIV-1 TATA box (7). Quantitative DNase I footprint titration experiments showed that polyamide 1 binds this sequence with an equilibrium dissociation constant (K_d) of 0.05 nM (7). Mismatch control polyamide 2 (ImIm-β-ImIm-γ-PyPy-β-PyPy-β-Dp; Fig. 1A), which differs from polyamide 1 only in the placement of the Py and Im amino acids, binds this DNA with 100-fold-reduced affinity relative to polyamide 1. No inhibition of TBP binding was observed for mismatch polyamide 2 over the polyamide concentration ranged tested (7). We wished to examine the effect of polyamides bound at various distances from the TATA box on TBP binding. To this end, site-directed mutagenesis was used to generate binding sites for polyamide 3 (ImPy-β-PyIm-daba-PyIm-β-ImPy-β-Dp [daba, *R*-2,4-diaminobutyric acid]; Fig. 1A) at various distances (up to 20 bp) either upstream (U) or downstream (D) of the HIV-1 TATA box (Fig. 1B). According to the polyamide pairing rules (4), polyamide 3 binds the DNA sequence 5′-WGCWCGW-3′ (where W = A or T) in either a forward orientation (amino- to carboxy-terminal polyamide orientation relative to the 5′-to-3′ DNA sequence) or reverse (carboxy- to amino-terminal) orientation (Fig. 1A, bottom). The preference for forward or reverse binding is likely due to small energetic differences caused by the base composition of the flanking DNA sequence. The constructs shown in Fig. 1B are denoted relative to the first T of the TATA box (+1). For example, construct D+6 has the first nucleotide of the polyamide-binding site located at nucleotide position +6 downstream from T+1. DNase I footprint titrations revealed that polyamide 3 binds these constructs with K_ds ranging from 2.0 to 6.0 nM (Table 1). Representative examples of these footprint titrations are shown in Fig. 2A for the U+1 and U−10 constructs, and graphical representations of these titrations are shown in Fig. 2B. In addition to the engineered sites for polyamide 3, each of the constructs contains a match site for polyamide 3 at nucleotide positions −113 to −119 from the transcription start site in the wild-type HIV-1 promoter/enhancer sequence (5′-AGCTCGA-3′; read on the bottom strand). High-affinity binding to this site is also observed in the footprinting experiments (Fig. 2A).

To determine the exact location and orientation of the bound polyamide in the minor groove, site-specific oxidative cleavage of the DNA with polyamide 3-EDTA·Fe(II) (Fig. 1A) was employed (43). This DNA cleavage method relies on the

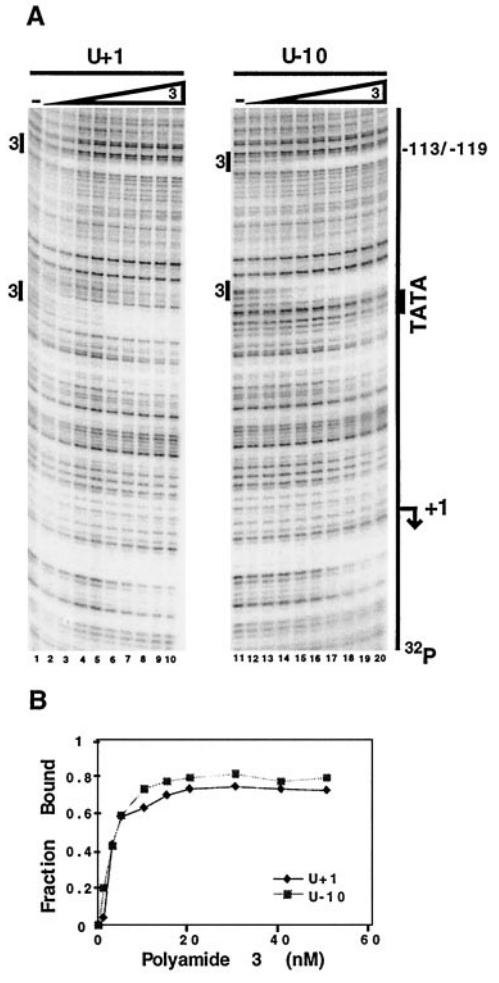

FIG. 2. DNase I footprint analysis of polyamide 3 binding. (A) DNase I footprint of two upstream constructs, U+1 (lanes 1 to 10) and U−10 (lanes 11 to 20). Lanes 1 and 11, DNA alone; lanes 2 to 10 and 12 to 20, polyamide 3 at 1, 3, 5, 10, 15, 20, 30, 40, and 50 nM, respectively. The locations of the polyamide binding sites, TATA box, transcription start site (denoted +1), and direction of transcription (arrow) are indicated. The match site at −113 to −119 is also indicated. ^{32}P, end label on the DNA probe. (B) Graphical representation of polyamide 3 titration plotted as the fraction of DNA bound (normalized to the fraction bound in the absence of polyamide) versus polyamide concentration.

generation of hydroxyl radicals by iron-mediated Fenton chemistry under reducing conditions. Since DNA cleavage occurs proximal to the polyamide-EDTA-tethered iron, the locations of cleavage sites thus determine the position and orientation of the bound polyamide (43). Figure 3A shows the affinity cleavage patterns with polyamide 3-EDTA · Fe(II) for each of the DNA constructs where polyamide sites are either adjacent to or overlap the TATA box. In each instance, the affinity cleavage pattern demonstrates binding to the engineered sites for polyamide 3 (Fig. 3B) and to the −113-to-−119 match site. Lower levels of DNA cleavage are observed at mismatch sites (such as at the polyamide 1 match site, 5′-AGCTGCA-3′, on the downstream side of the TATA box in U−1, U+1, and D+6). The affinity cleavage results are summarized in Fig. 3B. For some constructs, binding at the engineered sites is predominantly in the forward (N→C) orientation (U−1, U+1, and D+6). Note that there are two potential match sites for polyamide 3 in the U−1 construct (at nucleotides −10 to −4 on the top strand and at −7 to −1 on the bottom strand); however, phosphorimage analysis of the affinity cleavage reaction indicates a threefold-greater preference for the −7-to-−1 site than for the −10-to-−4 site. Binding in the reverse (C→N) orientation is observed for the D+8 construct, and both orientations are seen with the U−10 and U−15 constructs (data not shown). Polyamide orientations in these constructs can be explained by a preference for the polyamide to locate its carboxy-terminal Dp tail adjacent to an A · T base pair (4). These data confirm the presence of the polyamide at each of the engineered binding sites in these constructs.

We next monitored polyamide inhibition of TBP binding to each of the HIV-1 promoter constructs (Fig. 1B) using DNase I footprinting. Two examples of these experiments are shown in Fig. 4. TBP and polyamide 3 yield distinct footprints on these DNAs (Fig. 4A; compare lanes 3 and 4) such that displacement of TBP by the polyamide can be easily ascertained (such as for the D+6 construct; Fig. 4A). Graphical representations of the data for each of the constructs are shown in Fig. 5A and B, and 50% inhibitory concentration (IC_{50}) values obtained from these titrations are given in Table 1. The IC_{50} values observed for constructs U−2, U−1, U+1, and D+6 range from 1.7- to 3.8-fold higher than the K_ds for polyamide 3 binding to each of these constructs (Table 1). Polyamide 3 is an effective inhibitor of TBP binding when the 3′ terminus of its binding site is located either at nucleotide position +1 of the TATA box (U+1) or up to 2 bp upstream (U−2); however, no inhibition is observed when the binding site is 10 bp upstream (U−10; Fig. 5A). From affinity cleavage experiments (Fig. 3 and 1B), we conclude that polyamide 3 points in opposite orientations on the U−1 and U+1 constructs. For U−1, the Dp tail likely extends into the TATA box at T+1, while the charged turn amino acid contacts this base pair on the U+1 construct. Since similar IC_{50} values for TBP inhibition were obtained with these DNAs (Table 1), this suggests that polyamide orientation is not likely to be a critical factor for inhibition of TBP binding, at least on the upstream side of the TATA box.

Based on the crystal structure of the TBP-DNA complex (24, 25), the full extent of the binding site for TBP is the 8-bp DNA sequence shown in Fig. 1B. Thus, in constructs D+6 and D+8, the polyamide-binding site overlaps the TATA box, and consequently polyamide 3 inhibits TBP binding to these DNAs (Fig. 5B). Inhibition is observed at lower polyamide concentrations with the D+6 construct than with the D+8 construct. Polyamide 3 fails to inhibit TBP binding when the polyamide site is placed as little as 2 bp downstream of the TATA box (D+10). This contrasts with inhibition when the polyamide-binding site is located 2 bp upstream of the TATA box (U−2). The structural basis for this difference in upstream versus downstream inhibition profiles is addressed below.

In the situations where polyamide 3 fails to inhibit TBP binding (U−20, U−15, U−10, D+10), DNase footprinting reveals a triple complex of TBP, polyamide 3, and the DNA. One such example of polyamide and TBP co-occupancy, for the D+10 construct, is shown in Fig. 4B. In this instance,

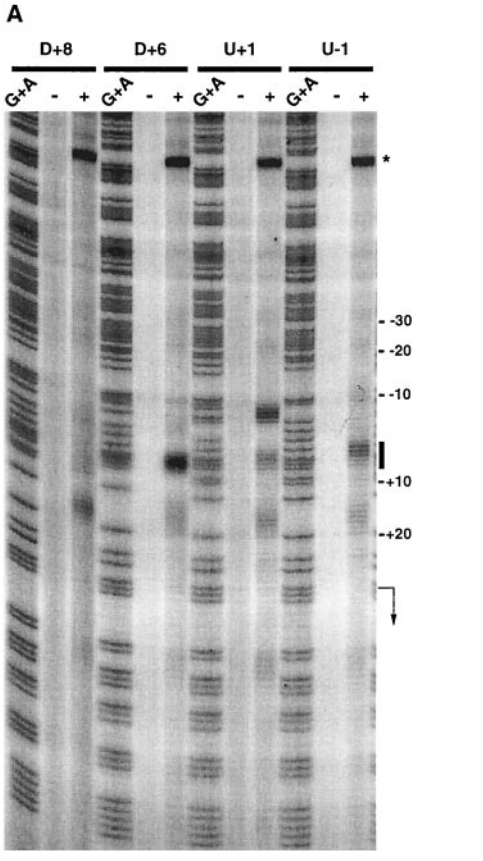

FIG. 3. Affinity cleavage with polyamide 3-EDTA·Fe(II). (A) Each of the indicated radiolabeled DNAs (at 40 pM) was incubated with polyamide at a final concentration of 5 nM (lanes +) or without polyamide (lanes −), and affinity cleavage reactions were performed as described in Materials and Methods. G+A sequencing reactions are also shown. The location of the TATA box (vertical bar) and nucleotide positions relative to T+1 of the TATA box are indicated. Arrow, location of the transcription start site and direction of transcription; *, match site at nucleotide positions −113 to −119, relative to the transcription start site, in each of the constructs. (B) DNA sequences of the HIV-1 promoter constructs (from nucleotide positions −44 to −6, with respect to the transcription start site). Polyamide-binding sites are in boldface, and the TATA sequence is boxed. Vertical lines, results for affinity cleavage with polyamide 3-EDTA·Fe(II), with the height and width of each line proportional to cleavage intensity at a given site.

protection from DNase I digestion across both the TATA box and the polyamide binding site is observed (Fig. 4B, lanes 8 to 10); however, close inspection of the TATA box region reveals a reduced occupancy by TBP in the presence of the polyamide (compare lane 4 with lanes 8 to 10). For the U−10 construct, in which the polyamide site is farther away from the TATA box, no decrease in TBP affinity was observed on polyamide binding (data not shown). We note that there is no correlation between polyamide binding affinity and the ability of the polyamide to inhibit TBP binding (Table 1). Thus, we conclude that the position of the polyamide-binding site relative to that of the TATA box and the upstream versus downstream location determine whether or not the polyamide will be inhibitory to TBP binding.

We also determined the K_ds for polyamide binding in the presence and absence of TBP to determine whether TBP affected the affinity of the polyamide for its target sequence. We found that polyamide-binding affinity was unaffected by the presence of TBP in the reaction mixtures, both for those constructs where polyamide 3 inhibited TBP binding and for those constructs where polyamide 3 and TBP co-occupied the DNA. An example of such polyamide-binding data is shown in Fig. 5C for the D+6 construct. Thus, TBP neither enhances polyamide binding nor acts as a competitive inhibitor of the polyamide.

Inhibition of the ternary TBP-TFIIA-DNA complex. We next examined whether polyamide 3 could inhibit formation of the ternary TBP-TFIIA-DNA complex. General transcription factor TFIIA has been shown to greatly stabilize the binary TBP-DNA complex (reviewed in references 33 and 39). Comparison of the DNase footprints of these binary and ternary complexes on the HIV-1 promoter clearly supports this view (compare

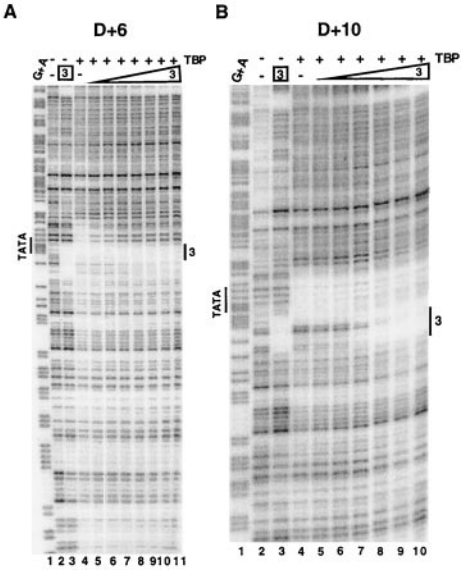

FIG. 4. Inhibition of TBP binding to the TATA box by polyamide 3. (A) DNase I footprint of the radiolabeled D+6 DNA in the presence of DNA alone (lane 2); 40 nM polyamide 3 (lane 3); TBP (lane 4); and TBP and polyamide 3 at 3, 5, 10, 15, 20, 30, and 40 nM (lanes 5 to 11, respectively). Lane 1, G+A sequencing ladder. (B) Co-occupancy of TBP and polyamide 3. DNase I footprint of D+10 in the presence of DNA alone (lane 2); 40 nM polyamide 3 (lane 3); TBP (lane 4); and TBP and polyamide 3 at 3, 5, 10, 20, 30, and 40 nM (lanes 5 to 10, respectively). Lane 1, G+A sequencing ladder.

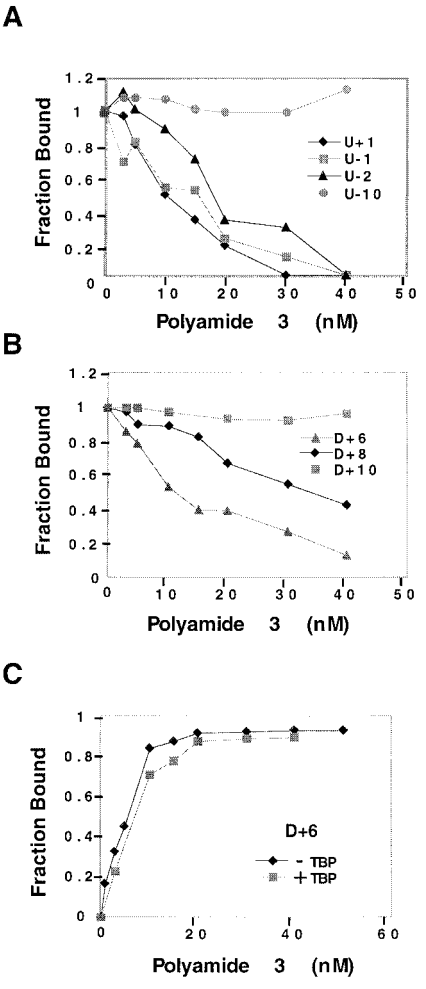

FIG. 5. The effects of distance on inhibition of TBP binding to the TATA box by polyamide 3. Shown is a graphical representation of footprint analysis of polyamide inhibition plotted as fraction of DNA bound (normalized to the fraction of DNA bound in the absence of polyamide) versus polyamide concentration. (A) Upstream constructs. (B) Downstream constructs. (C) Polyamide-binding affinity in the presence and absence of TBP for the D+6 construct.

lanes 3 and 4 of Fig. 6A). Far more protection of the DNA backbone is observed in the presence of TFIIA than with TBP alone even though a saturating concentration of TBP was used in these experiments. The crystal structure of the ternary complex shows that TFIIA interacts with the carboxy-terminal region of TBP, with the backbone of TATA box DNA, and with the 5′ flanking region of the TATA box (12, 38). Since TFIIA contacts the phosphodiester backbone of DNA upstream of the TATA box, we next asked whether polyamide 3 could inhibit formation of the TFIIA-TBP-DNA ternary complex on U−2 DNA (Fig. 6A, lanes 5 to 10). This construct was used since the polyamide-binding site is coincident with the contacts made by TFIIA in the ternary complex (12, 38). In this experiment, all reaction components were incubated simultaneously for 30 min prior to digestion with DNase I. Clearly, the TFIIA-TBP footprint (lane 4) changes to the polyamide footprint (lane 11) with increasing concentrations of polyamide 3. Figure 6B shows a graphical representation of the inhibition data for the binary TBP-DNA complex and for the ternary TBP-TFIIA-DNA complex. As expected from the relative stabilities of the binary and ternary complexes, an approximately two-fold-higher concentration of polyamide 3 is required for inhibition of the ternary TFIIA-TBP-DNA complex than for inhibition of the TBP-DNA complex. Nonetheless, polyamide 3 is an effective inhibitor of TBP-TFIIA-DNA complex formation.

Polyamide inhibition of transcription. Previous studies have established that polyamide 1, located adjacent to the TATA box (Fig. 1B), is an effective inhibitor of basal transcription from the HIV-1 promoter (7). We wished to know whether targeting sites distant from the TATA element with poly-

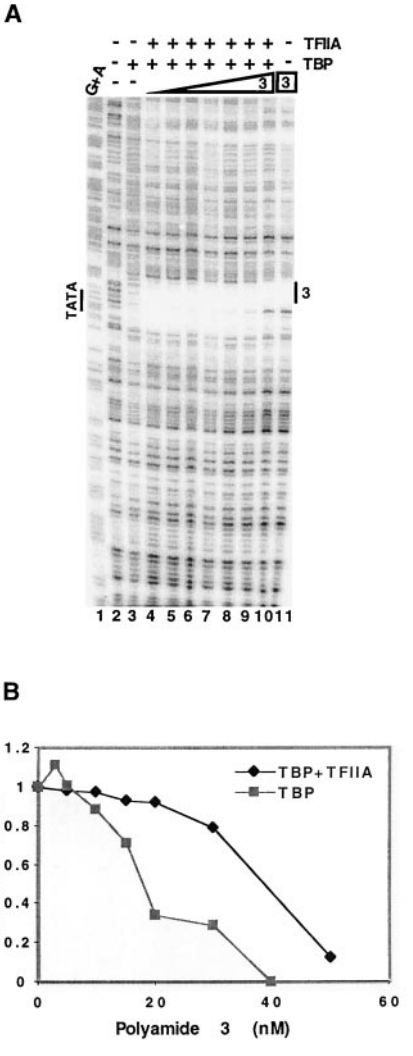

FIG. 6. Inhibition of the ternary TBP-TFIIA-DNA complex by polyamide 3. (A) DNase I footprint of U−2 DNA in the presence of DNA alone (lane 2); TBP (lane 3); TBP plus TFIIA (lane 4); TBP, TFIIA, and polyamide 3 at 3, 10, 15, 20, 30, and 50 nM (lanes 5 to 10, respectively). All reaction components were incubated simultaneously for 30 min prior to digestion with DNase. Lane 1, G+A sequencing ladder; lane 11, 50 nM polyomide 3, no TBP or TFIIA. The location of the TATA box and polyamide-binding site are indicated. (B) Graphical representation of inhibition plotted as the fraction of DNA bound (normalized to the fraction of TBP bound in the absence of polyamide) versus polyamide concentration.

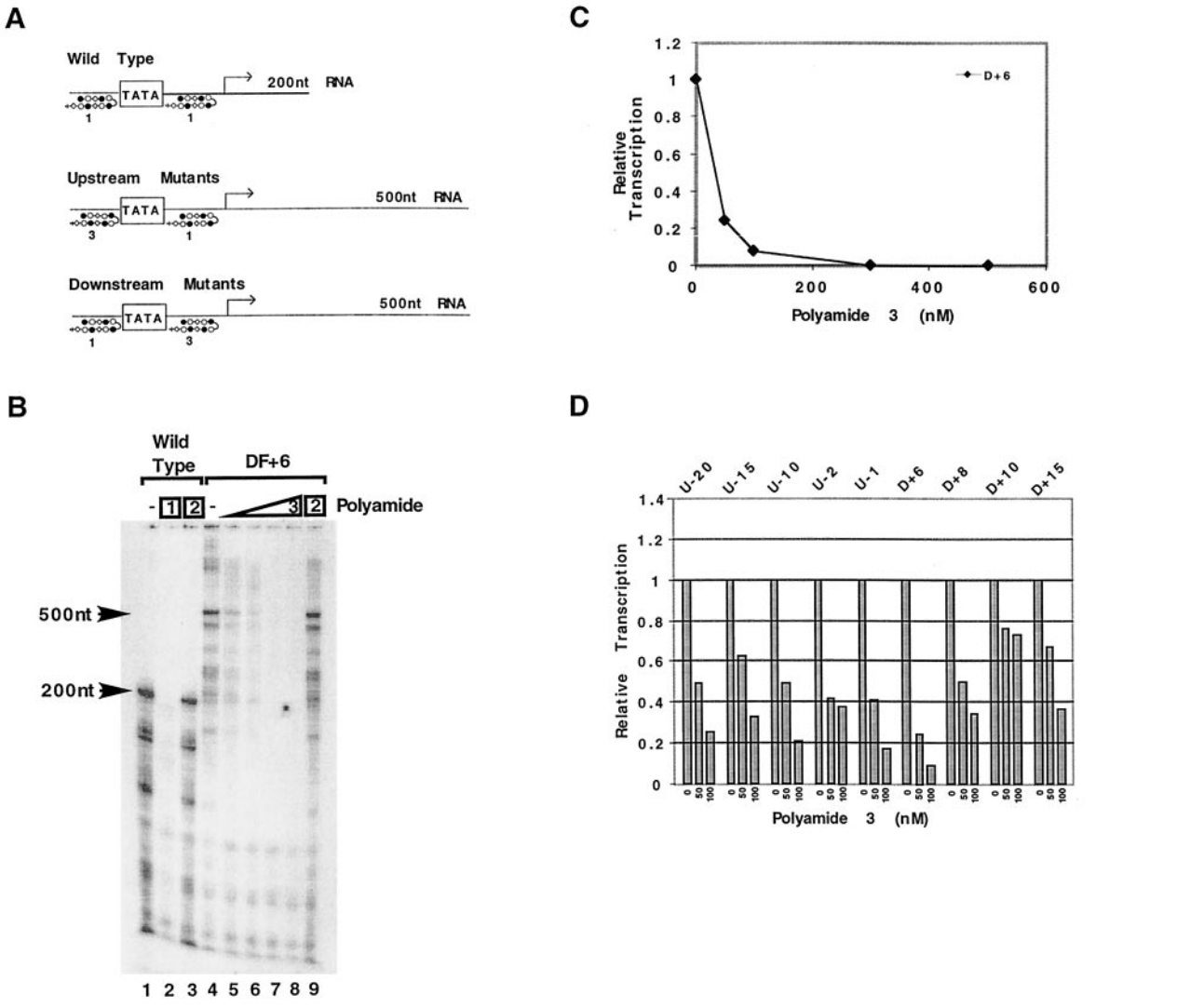

FIG. 7. Inhibition of basal transcription. (A) Schematic representation of wild-type and mutant construct transcripts. The polyamide binding sites, TATA box, and approximate transcription start sites are indicated as for Fig. 1. (B) Runoff transcription of wild-type and D+6 constructs monitored with a HeLa nuclear extract (see Materials and Methods). Lanes 1 to 3, wild-type DNA; lanes 4 to 9, D+6 DNA. The DNA was incubated with no polyamide (lane 1); 500 nM polyamide 1 (lane 2); 500 nM mismatch polyamide 2 (lane 3); no polyamide (lane 4); polyamide 3 at 50, 100, 300, and 500 nM (lanes 5 to 8, respectively); and 500 nM mismatch polyamide 2 (lane 9). (C) Graphical representation of inhibition plotted as percent transcription (normalized to the no-polyamide control reaction) versus polyamide concentration for D+6. (D) Relative transcription signals for each of the indicated DNA constructs (Fig. 1B) are plotted versus polyamide 3 concentration. Transcription levels for each template were normalized to the level observed in the absence of polyamide.

amides might also result in inhibition of transcription. To this end, we monitored the effect of polyamide 3 on basal transcription from each of the promoter constructs shown in Fig. 1B. For these experiments, we used a HeLa nuclear extract as a source of general transcription factors and RNA polymerase II for runoff transcription (Fig. 7). Digestion of the wild-type HIV-1 pLTR-CAT DNA with *Stu*I results in a template that generates an ~200-base RNA transcript, while digestion of the promoter mutant constructs with *Eco*RI results in templates that generate ~500-base transcripts (Fig. 7A and B). With the exception of U+1, each of the constructs supports basal HIV-1 transcription with activities ranging from 40 to 110% of that of the wild-type promoter (Table 1). These observations are in accord with previous studies with the HIV-1 promoter (20). The finding that the U+1 template failed to support transcription could reflect a deleterious effect of altering the DNA sequence immediately flanking the TATA box on binding one of the general transcription factors. Thus, this construct was not included in our polyamide transcription experiments.

Fig. 7B shows an example of a transcription inhibition experiment comparing the wild-type HIV-1 promoter with the D+6 construct. As expected (7), wild-type transcription is inhibited by match polyamide 1 (lane 2), while no inhibition is observed with mismatch polyamide 2 at the same polyamide concentration (500 nM; lane 3). Also as expected, polyamide 3 inhibits transcription from the D+6 template (lanes 5 to 8) and mismatch polyamide 2 does not (lane 9). The IC_{50} value observed in this experiment is approximately 20 nM (Fig. 7C;

Table 1). This concentration corresponds to an equimolar ratio of polyamide to binding sites in the transcription reaction mixture (24 nM sites). This calculation is based on the amount of DNA in the reaction mixture (100 ng of an 840-bp DNA template/25 μl reaction mixture) and the presence of three binding sites for polyamide 3 in the template DNA (two sites in the HIV-1 promoter and one in the chloramphenicol acetyltransferase gene).

Similar experiments were performed for each of the promoter constructs, and a graphical representation of the data is shown in Fig. 7D. IC_{50} values obtained from these and other experiments are listed in Table 1. Inhibition of transcription is achieved by targeting polyamide 3 to each of the DNA templates, with the exception of D+10. Notably, transcription from this template is only minimally affected by the polyamide, even at polyamide concentrations that result in severe inhibition from each of the other constructs. This result is not due to a decreased polyamide affinity for this DNA construct (Fig. 4B; Table 1), and this result has been obtained in four independent experiments (data not shown). These findings suggest that the binding of polyamide 3 to the minor groove immediately downstream of the TATA element fails to interfere with any required protein-DNA interaction necessary for basal transcription. In contrast, in situations where polyamide 3 either affects TBP binding (U−1, U−2, D + 6, and D + 8) or fails to affect TBP binding (U−10, etc.; Table 1), inhibition of transcription is observed. These observations suggest that sites of critical protein-DNA interactions are not simply restricted to the TATA box but rather lie both upstream and downstream of this sequence element. These contacts are unlikely to be highly DNA sequence specific since mutagenesis failed to uncover any critical sequences outside of the TATA element (Table 1) (20).

To insure that the results obtained with our series of mutant promoter constructs would also be true for the wild-type HIV-1 sequence, a polyamide was designed to bind a site overlapping the sequence bound by polyamide 3 in the D+15 construct. This polyamide, ImImPyPy-γ-PyPyImPy-β-Dp, binds the sequence 5′-TTGCCT-3′, located at nucleotide positions +17 to +22 downstream from T+1, and is also a potent inhibitor of transcription from the wild-type HIV-1 promoter (data not shown).

Inhibition of the TFIID-TFIIA-DNA complex. We wished to know whether the transcription inhibition we observe with constructs harboring polyamide sites distant from the TATA box might reflect inhibition of recruitment of one of the basal transcription factors to the HIV-1 promoter. One such factor is TFIID, which consists of TBP and TBP-associated factors (TAFs) (reviewed in references 16, 28, and 33). TFIID binding to core promoters is greatly stabilized by TFIIA, and such binding to the HIV-1 promoter has been demonstrated by gel mobility shift assays (22). DNase I footprinting demonstrates that TFIID binds over an extended region, generally spanning nucleotides −40 to +25 relative to the transcription start site (references 2 and 11 and references therein). For the HIV-1 promoter, DNase I footprinting experiments with HeLa nuclear extracts documented protein-DNA contacts over a similar region (15); however, no direct footprinting experiments on the HIV-1 promoter with purified TFIID have been presented.

To determine whether the inhibition of transcription observed with constructs containing polyamide binding sites distant from the TATA box may be due to inhibition of TFIID-DNA interactions, we used a gel mobility shift assay with the U−15 and D+15 constructs and highly purified TFIID and recombinant TFIIA. Human TFIID was immunopurified using an anti-hTAFII130 monoclonal antibody, washed extensively with solutions containing high concentrations of salt, and eluted from an antibody affinity resin with an epitope peptide (11). While this preparation of TFIID, in combination with TFIIA, has been shown to fully saturate a DNA fragment derived from the adenovirus major-late promoter (11), full protection of the HIV-1 probe was not observed in similar footprinting experiments (data not shown). Thus, we used EMSA to assess polyamide inhibition of TFIID and TFIIA binding to the HIV-1 promoter. Figure 8A and B demonstrates that polyamide 3 inhibits formation of this multiprotein complex on both the D+15 and U−15 DNAs, with IC_{50}s of approximately 150 and 50 nM, respectively, for these constructs (Fig. 8C). These IC_{50} values are similar to the IC_{50} for inhibition of transcription on these templates (75 nM; Table 1),

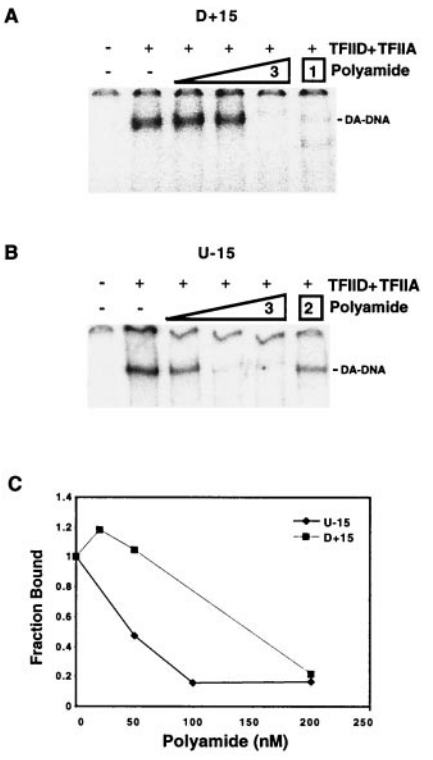

FIG. 8. Polyamide 3 inhibition of the TFIID-TFIIA-DNA complex analyzed by EMSA. (A) Radiolabeled D+15 DNA was incubated with either no polyamide (lanes −) or with 25, 50, and 200 nM polyamide 3 or 200 nM polyamide 1 for 15 min prior to the addition of TFIID plus TFIIA, as indicated. After a subsequent 20-min incubation, the samples were subjected to electrophoresis. Only the region of the gel containing the TFIID-TFIIA-DNA (DA-DNA) complex is shown. (B) Radiolabeled U−15 DNA was incubated with either no polyamide or with 50, 100, and 200 nM polyamide 3 or 200 nM polyamide 2 for 15 min prior to the addition of TFIID plus TFIIA, as for panel A. (C) Phosphorimage quantitation of the extent of DA-DNA complex formation with increasing concentrations of polyamide 3. Data are normalized to the phosphorimage units in the DA-DNA complex in the absence of polyamide.

suggesting that transcription inhibition is likely due to blocking TFIID and/or TFIIA access to these templates. As expected, polyamide 1, with a binding site on the upstream side of the TATA box in the D+15 construct, also inhibits formation of the TFIID-TFIIA-DNA complex (Fig. 8A). As a control, we found that mismatch polyamide 2 inhibits formation of the TFIID-TFIIA-DNA complex on the U−15 construct by only ~50% at a polyamide concentration where nearly complete inhibition is observed with match polyamide 3 (200 nM; Fig. 8B). These data suggest that transcription inhibition on the D+15 and U−15 constructs may be due to polyamide interference with recruitment of TFIID.

DISCUSSION

Py-Im polyamides have been used to inhibit the DNA binding activity of several classes of eukaryotic transcription factors (reviewed in reference 13). In the present study, we have shown that polyamides targeted to sequences either immediately upstream or downstream from the HIV-1 TATA element effectively inhibit TBP binding. Polyamides are effective inhibitors of TBP-DNA interactions when the binding site for the polyamide is close to or overlaps the TATA box. We suspect that polyamide inhibition of TBP binding could result from two possible mechanisms. For those polyamides that bind to sites overlapping the TATA box (U−1, U+1, D+6, and D+8), inhibition could be due to steric blockage of the minor groove. In these cases, the polyamide might interfere with insertion of amino acid side chains of TBP between base pair steps 1 and 2 and 7 and 8 of the 8-bp TATA element (24, 25). For U−2, where the binding site is 2 bp upstream of the TATA element, polyamide 3 binding might lock the DNA into a B-type structure that is incompatible with TBP binding. Cocrystal structures have shown that the Py-Im polyamides bind to undistorted B-type DNA (23) whereas TBP binding results in a large distortion of the double helix (24, 25). Thus, at saturating concentrations of polyamide, it is reasonable to suspect that the B-type polyamide-DNA complex predominates over the distorted TBP-DNA structure.

Surprisingly, a polyamide bound 2 bp downstream from the TATA element can co-occupy the DNA along with TBP (D+10; Fig. 4B), whereas a polyamide bound 2 bp upstream from the TATA box is inhibitory to TBP binding (Fig. 5A). This difference between upstream and downstream inhibition may be related to the fact that the majority of the binding energy for the TBP-DNA interaction comes from the interaction of the carboxy-terminal repeat region of TBP with the 5′ half of the TATA box (21). However, this interpretation assumes that the orientation of TBP in solution on the HIV-1 promoter is that found in the crystal structures (24, 25). Since affinity cleavage experiments suggest only a modest polarity for *Saccharomyces cerevisiae* TBP binding to the TATA element in solution (5), it may be that the HIV-1 TATA box DNA sequence itself imparts polarity to TBP binding. The adenovirus major-late promoter and cyc1 TATA box sequences used in the affinity cleavage experiments (5′-TATAAAAG-3′ and 5′-TATATAAA-3′, respectively) clearly differ from that of the HIV-1 TATA box (Fig. 1B). Additional biochemical data from DNA cleavage with the drug pluramycin (36) and transcription experiments (14) demonstrate that TBP can adopt an asymmetric orientation on some TATA sequences. One alternative explanation for upstream versus downstream inhibition is that the polyamide itself can orient TBP on the U+10 construct allowing co-occupancy; indeed, polyamide binding weakens the affinity of TBP somewhat on this construct (Fig. 4B). Additional experiments will be needed to resolve this issue.

We monitored the effect of polyamide 3 on basal transcription by RNA polymerase II from our series of DNA constructs in which the polyamide-binding site was located at various distances from the TATA box. Fifty percent inhibition of transcription was observed at an approximately equimolar ratio of polyamide to binding sites for those constructs that contained polyamide sites either adjacent to or overlapping the TATA element (Fig. 7D; Table 1). Inhibition of transcription from constructs such as U−2, U−1, D+6, and D+8 could simply be due to inhibition of the binding of the TBP subunit of TFIID (Fig. 6A and B). Additionally, it is well established that general transcription factors (GTFs) TFIIA and TFIIB contact promoter DNA both upstream and downstream of the TATA box (12, 26, 27, 38, 41), and transcription inhibition with some of our constructs could be due to steric clashes by the polyamide with these factors. Crystal structures of the core TFIIA-TBP-DNA complex reveal protein-DNA phosphate contacts both within and upstream of the TATA box (12, 38). The polyamide-binding site in the U−2 construct is coincident with upstream contacts made by TFIIA in the ternary complex. Although these contacts are located across the major groove, polyamide 3 might able to block TFIIA-DNA contacts by subtle changes in groove geometry (23). Indeed, we have shown that polyamide 3 can block the assembly of the TFIIA-TBP-DNA complex (Fig. 6).

For TFIIB, biochemical studies have identified a 7-bp TFIIB recognition element immediately upstream of the TATA box (26), and a cocrystal structure of the ternary TFIIB-TBP-DNA complex reveals that TFIIB contacts the major groove of DNA at this upstream site but also contacts both major and minor grooves downstream of the TATA box, extending to position +16 from T+1 (41). Interestingly, little or no transcription inhibition is observed with the D+10 construct although the minor-groove contacts made by TFIIB are well within the binding site for this polyamide. Additionally, photo-cross-linking experiments have identified TFIIA and TFIIB contacts within this region (27). We suggest that these downstream TFIIA- and TFIIB-DNA contacts are either not essential or at least not rate limiting for assembly of the transcription complex and basal transcription.

We also find transcription inhibition with constructs that harbor polyamide-binding sites further upstream and downstream from the TATA element (U−20, U−15, and D+15; Fig. 7D). Footprinting studies with HeLa nuclear extracts documented cellular protein-DNA interactions at these sites on the HIV-1 promoter (15, 19, 20). Candidate proteins for these interactions are the TAFs of TFIID for both the upstream and downstream contacts, TFIIAα for upstream contacts, and TFIIB for downstream contacts. Photo-cross-linking experiments demonstrate TFIIAα-DNA contacts upstream of the TATA box extending to −19 from T+1 of the TATA element and TFIIB contacts downstream to +18 (27). We find that polyamide 3 is a potent inhibitor of TFIID-TFIIA-DNA contacts on both the U−15 and D+15 constructs, with IC_{50} values

for inhibition of these protein-DNA interactions similar to those for inhibition of transcription (Fig. 8C and Table 1). Thus, inhibition of transcription with U−15 could be due to interference with either TAF- or TFIIA-DNA contacts and inhibition with D+15 may be due to interference with TAF-DNA contacts.

It is certainly possible that polyamides inhibit transcription by blocking the interaction of one of the other GTFs (TFIIE, -F, or -H) or RNA polymerase II with promoter DNA. Indeed, photo-cross-linking studies mapped the interactions of TFIIE, TFIIF, and RNA polymerase II with promoter DNA upstream from the transcription start site (3, 4, 34). Additionally, polyamides might prevent the bending and wrapping of the DNA around the GTFs or RNA polymerase, as proposed in a model for transcriptional regulation by Coulombe and Burton (3). In the present study, however, we considered TBP, TFIID, and TFIIA as potential candidates for interference by polyamides since these factors are among the first of the GTFs to bind the core promoter and since an inhibitor that blocks these interactions with DNA is expected to inhibit transcription from the targeted promoter. Thus, future studies will be needed to assess which of the GTFs or polymerase is the actual target for polyamide inhibition with each of the HIV-1 promoter constructs.

Our approach, of targeting DNA sequences within core promoters, might prove effective for inhibition of basal transcription from various mRNA-coding genes. The potential therapeutic applications of polyamide inhibition of gene transcription have been discussed previously (7). Previous mutagenesis studies of the HIV-1 promoter identified only the TATA box and sequences flanking the initiation site (−6 to +30) as important sequences for basal promoter activity (references 20 and 45 and references therein). However, the Py-Im polyamides clearly identify sites of important protein-DNA interactions that do not involve sequence-specific DNA interactions. Thus, our present results and our previous study with a tRNA gene (32) demonstrate that the Py-Im polyamides provide simple and convenient chemical probes for discovery of important protein-DNA contacts within a gene promoter.

ACKNOWLEDGMENTS

We thank Tae-Kyung Kim and D. Reinberg for the generous gift of TFIIA and Liliane Dickinson and E. Peter Geiduschek for discussions.

This work was supported by National Institutes of Health grants GM57148 to J.M.G. and P.B.D. and GM55235 to J.A.G. The Howard Hughes Medical Institute provided a predoctoral fellowship for E.E.B., and C.M. was supported by a postdoctoral fellowship from the NIH (GM19789).

REFERENCES

1. **Baird, E. E., and P. B. Dervan.** 1996. Solid phase synthesis of polyamides containing imidazole and pyrrole amino acids. J. Am. Chem. Soc. **118:**6141–6146.
2. **Chi, T., and M. Carey.** 1996. Assembly of the isomerized TFIIA–TFIID–TATA ternary complex is necessary and sufficient for gene activation. Genes Dev. **10:**2540–2550.
3. **Coulombe, B., and Z. F. Burton.** 1999. DNA bending and wrapping around RNA polymerase: a "revolutionary" model describing transcriptional mechanisms. Microbiol. Mol. Biol. Rev. **63:**457–478.
4. **Coulombe, B., J. Li, and J. Greenblatt.** 1994. Topological localization of the human transcription factors IIA, IIB, TATA box-binding protein, and RNA polymerase II-associated protein 30 on a class II promoter. J. Biol. Chem. **269:**19962–19967.
5. **Cox, J. M., M. M. Hayward, J. F. Sanchez, L. D. Gegnas, S. van der Zee, J. H. Dennis, P. B. Sigler, and A. Schepartz.** 1997. Bidirectional binding of the TATA box binding protein to the TATA box. Proc. Natl. Acad. Sci. USA **94:**13475–13480.
6. **Dervan, P. B., and R. W. Burli.** 1999. Sequence-specific DNA recognition by polyamides. Curr. Opin. Chem. Biol. **3:**688–693.
7. **Dickinson, L. A., R. J. Gulizia, J. W. Trauger, E. E. Baird, D. E. Mosier, J. M. Gottesfeld, and P. B. Dervan.** 1998. Inhibition of RNA polymerase II transcription in human cells by synthetic DNA-binding ligands. Proc. Natl. Acad. Sci. USA **95:**12890–12895.
8. **Dickinson, L. A., J. W. Trauger, E. E. Baird, P. B. Dervan, B. J. Graves, and J. M. Gottesfeld.** 1999. Inhibition of Ets-1 DNA binding and ternary complex formation between Ets-1, NF-kB, and DNA by a designed DNA-binding ligand. J. Biol. Chem. **274:**12765–12773.
9. **Dickinson, L. A., J. W. Trauger, E. E. Baird, P. Ghazal, P. B. Dervan, and J. M. Gottesfeld.** 1999. Anti-repression of RNA polymerase II transcription by pyrrole-imidazole polyamides. Biochemistry **38:**10801–10807.
10. **Dignam, J. D., P. L. Martin, B. S. Shastry, and R. G. Roeder.** 1983. Eucaryotic gene transcription with purified components. Methods Enzymol. **101:**582–598.
11. **Galasinski, S. K., T. N. Lively, A. De Barron, and J. A. Goodrich.** 2000. Acetyl coenzyme A stimulates RNA polymerase II transcription and promoter binding by transcription factor IID in the absence of histones. Mol. Cell. Biol. **20:**1923–1930.
12. **Geiger, J. H., S. Hahn, S. Lee, and P. B. Sigler.** 1996. Crystal structure of the yeast TFIIA/TBP/DNA complex. Science **272:**830–836.
13. **Gottesfeld, J. M., J. M. Turner, and P. B. Dervan.** 2000. Chemical approaches to control gene expression. Gene Expr. **9:**77–91.
14. **Grove, A., A. Galeone, E. Yu, L. Mayol, and E. P. Geiduschek.** 1998. Affinity, stability and polarity of binding of the TATA binding protein governed by flexure at the TATA box. J. Mol. Biol. **282:**731–739.
15. **Harrich, D., J. Garcia, F. Wu, R. Mitsuyasu, J. Gonazalez, and R. Gaynor.** 1989. Role of SP1-binding domains in in vivo transcriptional regulation of the human immunodeficiency virus type 1 long terminal repeat. J. Virol. **63:**2585–2591.
16. **Hernandez, N.** 1993. TBP, a universal eukaryotic transcription factor? Genes Dev. **7:**1291–1308.
17. **Janssen, S., O. Cuvier, M. Müller, and U. K. Laemmli.** 2000. Specific gain- and loss-of-function phenotypes induced by satellite-specific DNA-binding drugs fed to Drosophila melanogaster. Mol. Cell **6:**1013–1024.
18. **Janssen, S., T. Durussel, and U. K. Laemmli.** 2000. Chromatin opening of DNA satellites by targeted sequence-specific drugs. Mol. Cell **6:**999–1011.
19. **Jones, K. A., P. A. Luciw, and N. Duchange.** 1988. Structural arrangements of transcription control domains within the 5′-untranslated leader regions of the HIV-1 and HIV-2 promoters. Genes Dev. **2:**1101–1114.
20. **Jones, K. A., and B. M. Peterlin.** 1994. Control of RNA initiation and elongation at the HIV-1 promoter. Annu. Rev. Biochem. **63:**717–743.
21. **Juo, Z. S., T. K. Chiu, P. M. Leiberman, I. Baikalov, A. J. Berk, and R. E. Dickerson.** 1996. How proteins recognize the TATA box. J. Mol. Biol. **261:**239–254.
22. **Kashanchi, F., R. Shibata, E. K. Ross, J. N. Brady, and M. A. Martin.** 1994. Second-site long terminal repeat (LTR) revertants of replication-defective human immunodeficiency virus: effects of revertant TATA box motifs on virus infectivity, LTR-directed expression, in vitro RNA synthesis, and binding of basal transcription factors TFIID and TFIIA. J. Virol. **68:**3298–3307.
23. **Kielkopf, C. L., E. E. Baird, P. B. Dervan, and D. C. Rees.** 1998. Structural basis for GC recognition in the DNA minor groove. Nature Struct. Biol. **5:**104–109.
24. **Kim, J. L., D. B. Nikolov, and S. K. Burley.** 1993. Co-crystal structure of TBP recognizing the minor groove of a TATA element. Nature **365:**520–527.
25. **Kim, Y., J. H. Geiger, S. Hahn, and P. B. Sigler.** 1993. Crystal structure of a yeast TBP/TATA-box complex. Nature **365:**512–520.
26. **Lagrange, T., A. N. Kapanidis, H. Tang, D. Reinberg, and R. H. Ebright.** 1998. New core promoter element in RNA polymerase II-dependent transcription: sequence-specific DNA binding by transcription factor IIB. Genes Dev. **12:**34–44.
27. **Lagrange, T., T.-K. Kim, G. Orphanides, Y. W. Ebright, R. H. Ebright, and D. Reinberg.** 1996. High-resolution mapping of nucleoprotein complexes by site-specific protein-DNA photocrosslinking: organization of the human TBP-TFIIA-TFIIB-DNA quaternary complex. Proc. Natl. Acad. Sci. USA **93:**10620–10625.
28. **Lemon, B., and R. Tjian.** 2000. Orchestrated response: a symphony of transcription factors for gene control. Genes Dev. **14:**2551–2569.
29. **Lenzmeier, B. A., E. E. Baird, P. B. Dervan, and J. K. Nyborg.** 1999. The Tax protein-DNA interaction is essential for HTLV-I transactivation in vitro. J. Mol. Biol. **291:**731–744.
30. **Long, J. J., A. Leresche, R. W. Kriwacki, and J. M. Gottesfeld.** 1998. Repression of TFIIH transcriptional activity and TFIIH-associated cdk7 kinase activity at mitosis. Mol. Cell. Biol. **18:**1467–1476.
31. **Mapp, A. K., A. Z. Ansari, M. Ptashne, and P. B. Dervan.** 2000. Activation of gene expression by small molecule transcription factors. Proc. Natl. Acad. Sci. USA **97:**3930–3935.
32. **McBryant, S. J., E. E. Baird, J. W. Trauger, P. B. Dervan, and J. M. Gottesfeld.** 1999. Minor groove DNA-protein contacts upstream of a tRNA

gene detected with a synthetic DNA binding ligand. J. Mol. Biol. **286:**973–981.
33. **Orphanides, G., T. Lagrange, and D. Reinberg.** 1996. The general transcription factors of RNA polymerase II. Genes Dev. **10:**2657–2683.
34. **Robert, F., D. Forget, J. Li, J. Greenblatt, and B. Coulombe.** 1996. Localization of subunits of transcription factors IIE and IIF immediately upstream of the transcriptional initiation site of the adenovirus major late promoter. J. Biol. Chem. **271:**8517–8520.
35. **Sheridan, P. L., C. T. Sheline, K. Cannon, M. L. Voz, M. J. Pazin, J. T. Kadonaga, and K. A. Jones.** 1995. Activation of the HIV-1 enhancer by the LEF-1 HMG protein on nucleosome-assembled DNA in vitro. Genes Dev. **9:**2090–2104.
36. **Sun, D., and L. H. Hurley.** 1995. TBP binding to the TATA box induces a specific downstream unwinding site that is targeted by pluramycin. Chem. Biol. **2:**457–469.
37. **Sun, X., D. Ma, M. Sheldon, K. Yeung, and D. Reinberg.** 1994. Reconstitution of human TFIIA activity from recombinant polypeptides: a role in TFIID-mediated transcription. Genes Dev. **8:**2336–2348.
38. **Tan, S., Y. Hunziker, D. F. Sargent, and T. J. Richmond.** 1996. Crystal structure of a yeast TFIIA/TBP/DNA complex. Nature **381:**127–134.
39. **Tan, S., and T. J. Richmond.** 1998. Eukaryotic transcription factors. Curr. Opin. Struct. Biol. **8:**41–48.
40. **Trauger, J. W., E. E. Baird, and P. B. Dervan.** 1996. Subnanomolar sequence-specific recognition in the minor groove of DNA by designed ligands. Nature (London) **382:**559–561.
41. **Tsai, F. T. F., and P. B. Sigler.** 2000. Structural basis of preinitiation complex assembly on human pol II promoters. EMBO J. **19:**25–36.
42. **Turner, J. M., S. E. Swalley, E. E. Baird, and P. B. Dervan.** 1998. Aliphatic/aromatic amino acid pairings for polyamide recognition in the minor groove of DNA. J. Am. Chem. Soc. **120:**6219–6226.
43. **White, S., E. E. Baird, and P. B. Dervan.** 1997. On the pairing rules for recognition in the minor groove of DNA by pyrrole-imidazole polyamides. Chem. Biol. **4:**569–578.
44. **White, S., J. W. Szewczyk, J. M. Turner, E. E. Baird, and P. B. Dervan.** 1998. Recognition of the four Watson-Crick base pairs in the DNA minor groove by synthetic ligands. Nature (London) **391:**468–471.
45. **Zenzie-Gregory, B., P. Sheridan, K. A. Jones, and S. T. Smale.** 1993. HIV-1 core promoter lacks a simple initiator element but contains a bipartite activator at the transcription start site. J. Biol. Chem. **268:**15823–15832.